Biochemical Pharmacology xxx (2015) xxx–xxx

Contents lists available at ScienceDirect

Biochemical Pharmacology

journal homepage: www.elsevier.com/locate/biochempharm

Development and mechanism investigation of a new piperlongumine derivative as a potent anti-inflammatory agent

Lan-Di Sun, Fu Wang, Fang Dai, Yi-Hua Wang, Dong Lin, Bo Zhou *

State Key Laboratory of Applied Organic Chemistry, Lanzhou University, 222 Tianshui Street S., Lanzhou 730000, Gansu, China

ARTICLE INFO

Article history:
Received 15 February 2015
Accepted 26 March 2015
Available online xxx

Chemical compounds studied in this article:
Piperlongumine (PubChem CID: 637858)

Keywords:
Piperlongumine
Inflammation
Mechanism
NF-κB
MAPK
Autophagy

ABSTRACT

Inflammation, especially chronic inflammation, is directly involvement in the pathogenesis of many diseases including cancer. An effective approach for managing inflammation is to employ chemicals to block activation of nuclear factor-κB (NF-κB), a key regulator for inflammatory processes. Piperlongumine (piplartine, **PL**), an electrophilic molecule isolated from *Piper longum* L., possesses excellent anti-cancer and anti-inflammatory properties. In this study, a new **PL** analogue (**PL-0N**) was designed by replacing nitrogen atom of lactam in **PL** with carbon atom to increase its electrophilicity and thus anti-inflammatory activity. It was found that **PL-0N** is more potent than the parent compound in suppressing lipopolysaccharide (LPS)-induced secretion of nitric oxide and prostaglandin E_2 as well as expression of inducible nitric oxide synthase and cyclooxygenase-2 in RAW264.7 macrophages. Mechanistic investigation implies that **PL-0N** exerts anti-inflammatory activity through inhibition of LPS-induced NF-κB transduction pathway, down-regulation of LPS-induced MAPKs activation and impairment of proteasomal activity, but also enhancement of LPS-induced autophagy; the inhibition of NF-κB by **PL-0N** is achieved at various stages by: (i) preventing phosphorylation of IKKα/β, (ii) stabilizing the suppressor protein IκBα, (iii) interfering with the nuclear translocation of NF-κB, and (iv) inhibiting the DNA-binding of NF-κB. These data indicate that nitrogen-atom-lacking pattern is a successful strategy to improve anti-inflammatory property of **PL**, and that the novel molecule, PL-0N may be served as a promising lead for developing natural product-directed anti-inflammatory agents.

1. Introduction

Inflammation is a protective attempt of host defense against injury or infection, and begins the healing process. However, when inflammation becomes chronic, it has been proven harmful and may lead to a host of diseases, such as arthritis, atherosclerosis, and even cancer [1–3]. Nuclear factor-κB (NF-κB) is a key activator in inflammatory processes, its activity modulation is thus crucial for various inflammatory responses [4–6].

The NF-κB family comprises five members shared a conserved Rel homology domain (RHD), that is, p105/p50 (NF-κB1), p100/p52 (NF-κB2), p65 (RelA), RelB and c-Rel. In non-stimulated cells, homo- or hetero-dimers of these members are typically sequestered in the cytoplasm through interaction with its inhibitory kappa B (IκB), which specifically binds to NF-κB and masks its nuclear localization signals [7,8]. A large number of stimuli such as lipopolysaccharide (LPS), tumor necrosis factor (TNF)-α or interleukin (IL)-1β can trigger the activation of IκB kinase (IKK), which in turn phosphorylates IκB and results in its ubiquitination and degradation by the proteasome, allowing the liberated NF-κB to translocate into the nucleus. Once in the nucleus, the NF-κB acts as a transcriptional factor to regulate transcription of diverse genes encoding cytokines, inflammatory mediators and growth factors.

It has long been recognized that employing chemicals to inhibit inflammation is an effective method to alleviate the symptoms of inflammation-related diseases [9,10]. Many electrophilic natural products containing Michael acceptors, such as α,β-unsaturated ketone and α,β-unsaturated amide, have been shown to possess a variety of significant biological activities including anti-cancer and anti-inflammation activities [11]. Piperlongumine (PL) (Fig. 1A), an alkaloid isolated from *Piper longum* L., chemically characterized by the presence of two α, β-unsaturated imide functionalities and has been proved to be a promising anticancer molecular by targeting reactive oxygen species stress-response pathway [12]. In addition, **PL**-dependent anticancer activity involves cell cycle arrest, activation of caspases and mitogen-activated protein kinases (MAPKs), as well as down-regulation of anti-apoptotic proteins such as Bcl-2 and NF-κB [13–17]. Therefore, recent years have

* Corresponding author. Tel.: +86 931 8912500; fax: +86 931 8915557.
E-mail address: bozhou@lzu.edu.cn (B. Zhou).

http://dx.doi.org/10.1016/j.bcp.2015.03.014
0006-2952/

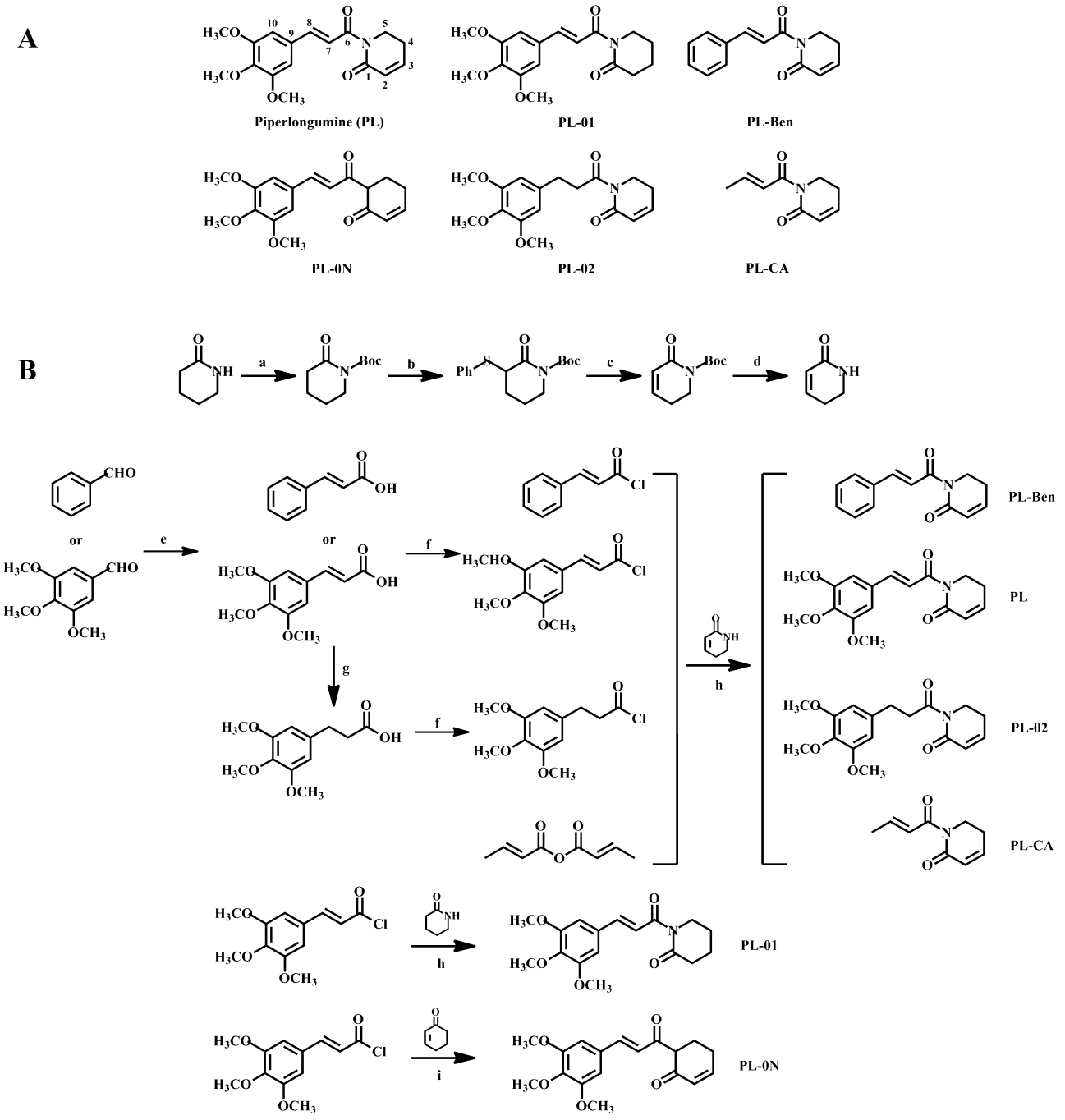

Fig. 1. Molecular structures (A) and synthesis (B) of piperlongumine and its designed analogs. For (B), reagents and conditions: (a) $(Boc)_2O$, TEA, DMAP, CH_2Cl_2, r.t., 3 h; (b) (i) LDA, THF, −78–0 °C, 45 min, (ii) PhSSPh, −78 °C—r.t., 5 h; (c) (i) m-CPBA, CH_2Cl_2, −78–0 °C, (ii) $CaCO_3$, CCl_4, reflux; (d) CF_3COOH, CH_2Cl_2, r.t.; (e) Py, Piperidine, 95–100 °C, 3 h; (f) $SOCl_2$, CH_2Cl_2, reflux, 4 h; (g) Pd/C, H_2, r.t., 24 h; (h) NaH, THF, 0 °C—r.t., 18–24 h; (i) LDA/THF, −78 °C.

witnessed a growing interest in modifying the molecular structure of **PL** to improve its biological functions [18,19]. We believe that its electrophilicity resulting from the two Michael acceptors is vital for maintaining its biological functions as evidenced by a pioneer study on anticancer activity of **PL** and its analogs [18]. From a chemical point of view, a replacement of nitrogen atom of lactam in **PL** with carbon atom helps to improve its electrophilicity. Thus, as part of our ongoing research project on anticancer lead-finding from natural products [20,21], we synthesized a nitrogen-atom-lacking analog of **PL** (**PL-0N**) (Fig. 1A) to find a more important anti-inflammatory agent than this parent molecular and investigate its action mechanisms. At the same time, to clarify the importance of the electrophilicity and the structure requirement of **PL** for its anti-inflammatory activity, we also designed and synthesized a few other analogs, where the Michael acceptors are partially reduced (**PL-01** and **PL-02**) (Fig. 1A) or the three methoxyl groups and the aromatic ring are removed as exemplified by **PL-Ben** and **PL-CA**, respectively (Fig. 1A).

Our work suggests that the Michael acceptor moiety in **PL** plays an important role in its anti-inflammatory activity and the replacement of nitrogen atom of lactam by carbon atom increases effectively this activity. Investigation of mechanisms underlying anti-inflammatory activity of **PL-0N** shows that it prevents the expression of inducible nitric oxide synthase (iNOS) and cyclooxygenase-2 (COX-2) and production of nitric oxide (NO) and prostaglandin E_2 (PGE_2) by inhibiting LPS-induced NF-κB signaling

Please cite this article in press as: Sun L-D, et al. Development and mechanism investigation of a new piperlongumine derivative as a potent anti-inflammatory agent. Biochem Pharmacol (2015), http://dx.doi.org/10.1016/j.bcp.2015.03.014

pathway and MAPKs activation, as well as impairing proteasome activity, but also enhancing LPS-induced autophagy in macrophage RAW264.7 cells.

2. Materials and methods

2.1. Materials

3-(4,5-Dimethylthiazol-2-yl)-2,5-diphenyltetrazolium bromide (MTT) was purchased from Amresco, Inc. (Solon, OH, USA). LPS from *Escherichia coli* 0111:B4, Sulfanilamide, *N*-(1-naphthyl) ethylenediamine dihydrochloride, 3-methyladenine (3-MA) and the primary antibody against LC3B were obtained from Sigma-Aldrich Co. LLC. (St. Louis, MO, USA). Dulbecco's modified eagle medium (DMEM) was obtained from Life Technologies Corp. (Grand Island, NY, USA). The primary antibodies against iNOS, COX-2, p50, p65, IκBα, p-IκBα, IKKβ, p-IKKα/β, p38, p-p38, JNK, p-JNK, ERK1/2, p-ERK1/2, TAK1, p-TAK1, TAB2, mTOR, p-mTOR, Akt and p-Akt were purchased from Cell Signaling Technology, Inc. (Beverly, MA, USA). The primary antibody against p62 was purchased from BD biosciences (San Jose, CA, USA). The primary antibodies against β-Actin and Lamin A and Protein A/G PLUS-Agarose were purchased from Santa Cruz Biotechnology, Inc. (Santa Cruz, CA, USA). HRP-labeled secondary antibody was obtained from TransGen Biotech Co., Ltd. (Beijing, China). Alexa Fluor 488-labeled goat anti-rabbit IgG and 4′,6-diamidino-2-phenylindole (DAPI) were purchased from Beyotime Institute of Biotechnology (Jingsu, China). Fluorogenic peptide substrates Suc-LLVY-AMC, Z-LLE-AMC and Z-ARR-AMC were obtained from Calbiochem, Inc. (San Diego, CA, USA). Specific pharmacological antagonists SB203580 and U0126 were purchased from Cell Signaling Technology, and SP600125 was from Sigma-Aldrich. Rapamycin was purchased from Selleck Chemicals (Houston, TX, USA). All other chemicals were of analytical grade.

2.2. Synthesis of **PL** and its designed analogs

Synthesis of **PL** and its designed analogs was conducted according to the route described in Fig. 1B. ^{1}H and ^{13}C NMR spectra were recorded on a Bruker AVANCE III 400 MHz NMR spectrometer (Bruker Daltonic Inc., Bremen, Germany). The electron spray ionization mass spectra (ESI-MS) were measured on a Bruker micrOTOF II mass spectrometer (Bruker Daltonic Inc., Bremen, Germany). The electron ionization mass spectra (EI-MS) were obtained on a Trace GC Ultra & DSQ mass spectrometer (Thermo scientific Inc., Allured, Illinois, USA). High resolution mass spectra (HRMS) were recorded on a Bruker APEX II 47e mass spectrometer (Bruker Daltonic Inc., Bremen, Germany).

2.2.1. Synthesis of tert-butyl-2-oxopiperidine-1-carboxylate [22]

Triethylamine (13.6 mL, 97.8 mmol), 4-dimethylaminopyridine (DMAP)(1.20 g, 9.78 mmol) and di-*tert*-butyl dicarbonate (32.0 g, 147 mmol) were added to a stirring solution of δ-valerolactam (9.69 g, 97.8 mmol) in CH_2Cl_2 (150 mL). The solution was stirred at room temperature for 3 h. The reaction mixture was then concentrated under reduced pressure to give an orange semi-solid. The semi-solid was dispersed into CH_2Cl_2 and purified by column chromatography (silica gel, diethyl ether/hexanes 3:1) to yield *tert*-butyl-2-oxopiperidine-1-carboxylate, a white crystalline solid (18 g, 90.4%).

2.2.2. Synthesis of tert-butyl 2-oxo-3-(phenylthio)piperidine-1-carboxylate [23]

To a stirring solution of *tert*-butyl-2-oxopiperidine-1-carboxylate (4.0 g, 20.1 mmol) in tetrahydrofuran (THF) (20 mL) was added dropwise Lithium diisopropylamide (LDA) (11.0 mL, 22.1 mmol) under stirring at −78 °C. The mixture was stirred at −78 °C for 45 min, and then a solution of 4.82 g (22.1 mmol) diphenyl disulfide in THF (10 mL) was added to the reaction system at −78 °C. The reaction was maintained for 2 h at −78 °C and allowed to warm up to 0 °C, continuing to stir for 3 h. The reaction was then quenched with H_2O (10 mL), diluted using water and extracted with CH_2Cl_2 (3 × 80 mL). The organic layers were combined, washed with brine (80 mL) and dried over $MgSO_4$, filtered and concentrated to form an orange oil. The oil was dissolved in CH_2Cl_2 and purified by flash column chromatography on silica gel (petroleum/ethyl acetate 4:1) to provide *tert*-butyl 2-oxo-3-(phenylthio)piperidine-1-carboxylate as a colorless oil (2.80 g, 45.4%).

2.2.3. Synthesis of tert-butyl 2-oxo-5,6-dihydropyridine-1(2H)-carboxylate [23,24]

m-Chloroperbenzoic acid (90%) (1.81 g, 9.45 mmol) was added portion-wise to a solution of *tert*-butyl 2-oxo-3-(phenylthio)piperidine-1-carboxylate (2.76 g, 9 mmol) in 100 mL of CH_2Cl_2 at −78 °C. The solution was stirred for 1 h at −78 °C, followed by addition of saturated $NaHCO_3$ solution (80 mL), and then warmed up to 0 °C for 30 min. The organic phase was separated and the aqueous layer was extracted with CH_2Cl_2 (2 × 60 mL). The combined organic phase was dried over anhydrous Na_2SO_4 and removed the solvent. $CaCO_3$ (0.912 g, 9.12 mmol) was added to the residue in CCl_4 (100 mL) and refluxed for 4 h. The reaction mixture was cooled to room temperature, filtered calcium carbonate and washed with CH_2Cl_2 (2 × 40 mL). The combined organic phases was washed with brine (80 mL), dried over anhydrous Na_2SO_4, filtered and concentrated. The residue oil was refined by flash column chromatography (petroleum ether/ethyl acetate 6:1 to 3:1) to provide *tert*-butyl 2-oxo-5,6-dihydropyridine-1(2*H*)-carboxylate as a colorless oil (1.104 g, 61.5%).

2.2.4. Synthesis of 5,6-dihydropyridin-2(1H)-one [22]

To a solution of amide tert-butyl 2-oxo-5,6-dihydropyridine-1(2*H*)-carboxylate (1.576 g, 8 mmol) in CH_2Cl_2 (10 mL) was added dropwise trifluoroacetic acid (8 mL). The mixture was allowed to stir at room temperature for 1 h. Toluene (20 mL) was added to the reaction mixture and the solution was concentrated under reduced pressure to give a light yellow oil. The oil was then dissolved in CH_2Cl_2 (50 mL) and washed with an aqueous saturated solution of K_2CO_3 (40 mL). The aqueous layer was then extracted with CH_2Cl_2/CH_3OH (10/1) (4 × 50 mL). The organic layers were then combined, dried over $MgSO_4$, filtered and concentrated under reduced pressure. The crude product was further purified by flash column chromatography (petroleum ether/ethyl acetate) to give a white solid 5,6-dihydropyridin-2(1*H*)-one (0.66 g, 85%).

2.2.5. Synthesis of substituted acrylic acid [25]

Malonic acid (12 mmol) was added to a mixture of substituted aryl aldehyde (10 mmol), pyridine (6 mL) and piperidine (0.6 mL). The reaction was heated to 95–100 °C and stirred for 3 h, then cooling for 10 min. The solution was poured into 10 mol/L hydrochloric acid solution (80 mL) at 0 °C to produce white solid after standing for half an hour. The solid was filtered, washed several times with water, and dried under vacuum to give product substituted acrylic acid.

2.2.6. Synthesis of 3-(3,4,5-trimethoxyphenyl)propionic acid [26]

Palladium 10% on carbon (0.3 g) was added to the solution of 3-(3,4,5-trimethoxyphenyl) acrylic acid in 60 mL of absolute ethanol. The air molecules in the reactor were evacuated by vacuum pump, and hydrogen was introduced into reactor with a balloon as buffer. The reaction was stirred at room temperature for 24 h, and then the catalysts were filtered away. The reaction mixture washed with ethanol. Combined organic phases were concentrated to obtain a white crude product, which was further

Please cite this article in press as: Sun L-D, et al. Development and mechanism investigation of a new piperlongumine derivative as a potent anti-inflammatory agent. Biochem Pharmacol (2015), http://dx.doi.org/10.1016/j.bcp.2015.03.014

purified by recrystallization with methanol and water to give 3-(3,4,5-trimethoxyphenyl)propionic acid as a white crystal (3.28 g, 91%).

2.2.7. Synthesis of substituted acryloyl chloride [27]

Thionyl chloride (0.65 mL, 9 mmol) was added to a solution of substituted acrylic acid (3 mmol) in CH_2Cl_2 (6 mL). The reaction was stirred and refluxed for 4 h under dry condition. The solution was concentrated under reduced pressure to give a light yellow solid or colorless oil substituted acryloyl chloride. The synthesized substituted acryloyl chloride was directly used in the subsequent reactions without further purification.

*2.2.8. Synthesis of piperlongumine and its analogs (**PL**, **PL-01**, **PL-02**, **PL-Ben**, **PL-CA**)*

The corresponding acyl chloride (or acid anhydride) (3 mmol) was added to a solution of δ-valerolactam or 5,6-dihydropyridin-2(1*H*)-one (3.3 mmol) in 15 mL of THF. The system was cooled to 0 °C with ice water and NaH (3.3 mmol) was slowly added to the reaction mixture. The reaction was continued at 0 °C for 2 h and then stirred for 18–24 h at room temperature under dry air. The solution was poured into appropriate ice water, stirred for a few minutes and extracted with ethyl acetate. Combined organic phases were dried and concentrated. Purification was performed by flash column chromatography (petroleum ether/ethyl acetate) to give the corresponding analogs.

*2.2.9. Synthesis of (E)-6-(3-(3,4,5-trimethoxyphenyl)acryloyl)cyclohex-2-enone (**PL-0N**) [28]*

Cyclohex-2-enone (0.48 g, 6 mmol) was dissolved in 15 mL of THF, and the solution was stirred and cooled to −78 °C under dry nitrogen. Then LDA (6.6 mmol in THF) was dropped to the system by syringe, stirring the system for 45 min under −78 °C. The acyl chloride (3 mmol) dispersed into 15 mL of THF was slowly added to the reaction mixture, and the reaction was continued for 1 h at same temperature then 1 h at 0 °C. 10 mL of water was used to terminate the reaction and appropriate water was poured into the reaction system again. The system was stood for a while, and then water phase was separated from the system and extracted by ethyl acetate. Combined organic phases were washed using brine, dried over anhydrous Na_2SO_4 and concentrated by rotary evaporator. Crude product was purified by flash column chromatography (petroleum ether/ethyl acetate) to give yellow **PL-0N**.

*2.2.10. (E)-1-(3-(3,4,5-Trimethoxyphenyl)acryloyl)-5,6-dihydropyridin-2(1H)-one (**PL**)*

White solid, yield 72%; **^{1}H NMR** (400 MHz, $CDCl_3$): δ = 7.68 (d, *J* = 15.6 Hz, 1*H*), 7.43 (d, *J* = 15.6 Hz, 1*H*), 6.98–6.93 (m, 1*H*), 6.81 (s, 2*H*), 6.06 (d, *J* = 9.6 Hz, 1*H*), 4.05 (t, *J* = 6.4 Hz, 2*H*), 3.90 (s, 6*H*), 3.88 (s, 3*H*), 2.51–2.47 (m, 2*H*); **^{13}C NMR** (100 MHz, $CDCl_3$): δ = 168.9, 165.8, 153.3, 145.5, 143.8, 139.9, 130.6, 125.8, 121.0, 60.9, 56.1, 56.1, 41.6, 24.8; **MS** (EI): (*m*/*z*) = 318.3 $[M + H]^+$.

*2.2.11. (E)-1-(3-(3,4,5-Trimethoxyphenyl)acryloyl)piperidin-2-one (**PL-01**)*

White solid, yield 65.1%; **^{1}H NMR** (400 MHz, $CDCl_3$): δ = 7.64 (d, *J* = 15.4 Hz, 1*H*), 7.36 (d, *J* = 15.4 Hz, 1*H*), 6.79 (s, 2*H*), 3.89 (s, 6*H*), 3.87 (s, 3*H*), 3.80 (t, *J* = 6.0 Hz, 2*H*), 2.63–2.60 (m, 2*H*), 1.91–1.88 (m, 4*H*); **^{13}C NMR** (100 MHz, $CDCl_3$): δ = 173.9, 169.6, 153.3, 143.4, 139.9, 130.6, 121.3, 105.4, 60.9, 56.1, 44.6, 34.9, 22.5, 20.6; **MS** (ESI): (*m*/*z*) = 319.9 $[M + H]^+$.

*2.2.12. (E)-1-(3-(3,4,5-Trimethoxyphenyl)acryloyl)piperidin-2-one (**PL-02**)*

White solid, yield 37.2%; **^{1}H NMR** (400 MHz, $CDCl_3$): δ = 6.89 (dt, *J* = 9.6, 4.0 Hz, 1*H*), 6.47 (s, 2*H*), 6.00 (dt, *J* = 9.6, 2.0 Hz, 1*H*), 3.98 (t, *J* = 6.4 Hz, 1*H*), 3.85 (s, 6*H*), 3.82 (s, 3*H*), 3.25 (t, *J* = 8.0 Hz, 2*H*), 2.94 (t, *J* = 8.0 Hz, 2*H*), 2.42–2.37 (m, 2*H*); **^{13}C NMR** (100 MHz, $CDCl_3$) δ = 175.5, 165.3, 153.0, 145.2, 136.9, 136.2, 125.8, 105.4, 60.8, 56.0, 40.9, 31.5, 24.6; **HRMS** (ESI): *m*/*z* calculated for $[M + H]^+$: 320.1492. Found: 320.1488, error = 1.2 ppm.

*2.2.13. 1-Cinnamoyl-5,6-dihydropyridin-2(1H)-one (**PL-Ben**)*

White solid, yield 26.8%; **^{1}H NMR** (400 MHz, $CDCl_3$): δ = 7.76 (d, *J* = 16.0 Hz, 1*H*), 7.60–7.56 (m, 2*H*), 7.52 (d, *J* = 16.0 Hz, 1*H*), 7.41–7.37 (m, 3*H*), 6.94 (dt, *J* = 9.6, 4.0 Hz, 1*H*), 6.05 (dt, *J* = 9.6, 1.6 Hz, 1*H*), 4.05 (t, *J* = 6.4 Hz, 2*H*), 2.50–2.46 (m, 2*H*); **^{13}C NMR** (100 MHz, $CDCl_3$): δ = 168.9, 165.8, 145.4, 143.6, 135.1, 130.0, 128.7, 128.3, 125.8, 121.8, 41.6, 24.8; **MS** (ESI): (*m*/*z*) = 228.1 $[M + H]^+$.

*2.2.14. (E)-6-(3-(3,4,5-Trimethoxyphenyl)acryloyl)cyclohex-2-enone (**PL-0N**)*

Yellow solid, yield 65.3%; **^{1}H NMR** (400 MHz, $CDCl_3$): δ = 7.55 (d, *J* = 15.6 Hz, 1*H*), 6.87–6.78 (m, 2*H*), 6.76 (s, 2*H*), 6.16 (dt, *J* = 9.6, 1.6 Hz, 1*H*), 3.90 (s, 6*H*), 3.88 (s, 3*H*), 2.76 (t, *J* = 7.2 Hz, 2*H*), 2.44–2.38 (m, 2*H*); **^{13}C NMR** (100 MHz, $CDCl_3$): δ = 190.1, 169.9, 153.4, 146.9, 139.7, 139.0, 131.2, 129.8, 117.7, 105.8, 105.0, 60.9, 56.2, 24.6, 22.0; **MS** (EI): (*m*/*z*) = 317.3$[M + H]^+$.

*2.2.15. (E)-1-(But-2-enoyl)-5,6-dihydropyridin-2(1H)-one (**PL-CA**)*

Liquid, yield 73%; **^{1}H NMR** (400 MHz, $CDCl_3$): δ = 7.06–6.96 (m, 1*H*), 6.94–6.77 (m, 1*H*), 6.00–5.94 (m, 1*H*), 3.97–3.90 (m, 2*H*), 2.43–2.40 (m, 2*H*), 1.92–1.86 (m, 3*H*); **^{13}C NMR** (100 MHz, $CDCl_3$): δ = 168.7, 165.6, 145.3, 143.4, 126.2, 125.7,41.4, 24.7, 18.2; **MS** (EI): (*m*/*z*) = 165 [M].

2.3. Cell culture

Murine macrophage RAW264.7 cells were obtained from Shanghai Institutes for Biological Sciences, Chinese Academy of Sciences, and grown at 37 °C in a humidified CO_2 (5%) incubator. The cells were maintained in DMEM medium supplemented with 10% heat-inactivated fetal bovine serum, 100 U/mL penicillin and 100 U/mL streptomycin.

2.4. Cell viability assay

Cell viability was evaluated by the MTT reduction assay. Briefly, the cells were seeded at a density of 8000 cells/well in 96-well plates and treated with the test compounds. After 24 h incubation, the medium was replaced by fresh medium containing 0.5 mg/mL MTT and the cells were incubated for 4 h at 37 °C. The dark blue formazan crystals formed in the cells were dissolved in 100 μL of DMSO, and then the absorbance was measured at 570 nm using a Bio-Rad M680 microplate reader (Bio-Rad Laboratories, Inc., Hercules, CA, USA).

2.5. Nitrite assay

The nitrite concentration in the culture medium was measured as an indicator of NO production based on the Griess reaction [29]. RAW264.7 cells (8×10^4 cells/well) were plated in 96-well plates for overnight and pretreated with the diverse compounds for 1 h, then stimulated with LPS for 18 h. Equal volumes (100 μL) of cultured medium and Griess reagent (1% Sulfanilamide in 5% phosphoric acid and 0.1% *N*-(1-naphthyl) ethylenediamine dihydrochloride in distilled water) were mixed in a 96-well plate and incubated for 10 min at room temperature. The optical density was read at 540 nm with a Tecan Infinite® 200 PRO multimode reader (Tecan Group Ltd., Männedorf, Switzerland), and nitrite concentration was calculated by comparison with a sodium nitrite solution standard curve.

Please cite this article in press as: Sun L-D, et al. Development and mechanism investigation of a new piperlongumine derivative as a potent anti-inflammatory agent. Biochem Pharmacol (2015), http://dx.doi.org/10.1016/j.bcp.2015.03.014

2.6. Determination of PGE_2 production

RAW264.7 cells (3×10^5 cells/well) were plated in 24-well plates for overnight and pretreated with the test compounds for 24 h with or without LPS. The PGE_2 concentration in the culture medium was quantified using a commercially available enzyme-linked immunosorbent assay (ELISA) kit (R&D Systems, Inc., Minneapolis, MN, USA) according to the manufacturer's instructions.

2.7. Protein preparation, immunoprecipitation, and Western blot analysis

Cells were harvested, washed two times with ice-cold phosphate-buffered saline and whole-cell and nuclear proteins were extracted according to the protocol of Western and IP lysis buffer (Beyotime Institute of Biotechnology) and Nuclear and Cytoplasmic Protein Extraction Kit (Viagene Biotech Inc., Beijing, China), respectively. For immunoprecipitation, equivalent amounts of whole-cell lysates were incubated with specific primary antibodies overnight at 4 °C under rotation. Protein A/G PLUS-Agarose was then added and incubated for an additional 4 h at 4 °C under rotation. The immunoprecipitated complexes were washed 5 times with Western and IP lysis buffer. For immunoblotting, the immunoprecipitates, proteins from whole-cell, nuclear or cytoplasm were separated on SDS-polyacrylamide gels and transferred onto the nitrocellulose membranes (Bio-Rad Laboratories, Inc.) or Immun-Blot™ PVDF membrane (Bio-Rad Laboratories, Inc.). The membranes were blocked with 5% skim milk in Tris buffered saline (TBS) containing 0.1% Tween-20, and probed for the protein of interest with a specific primary antibody before incubation with its corresponding HRP-conjugated secondary antibody. Blotted proteins were detected using the Image-Quant 400 capture imaging system (GE Healthcare, Little Chalfont, UK), and band intensities were quantified using Image J software (National Institutes of Health, Bethesda, MD, USA).

2.8. Electrophoretic mobility shift assay (EMSA) for NF-κB

The cells were pretreated with test compounds for 5 h and then stimulated with LPS (1 μg/mL) for another 30 min. The DNA binding activity of NF-κB was determined with a biotin-labeled oligonucleotide bio-NF-κB probe according to the manufacturer's instruction of EMSA kit (Viagene Biotech Inc.).

2.9. Immunofluorescence analysis

RAW264.7 cells were grown on glass coverslip in six-well plates, fixed with 4% paraformaldehyde (w/v) for 20 min at room temperature and blocked for 1 h with 5% BSA in TBS containing 0.1% Triton X-100. Then, the cells were incubated with a primary antibodies, followed by Alexa Fluor 488-labeled goat anti-rabbit IgG. After a wash step, they were stained with DAPI and the images were acquired.

2.10. Assays of proteasome activity

The various peptidase activities of the proteasome were measured using the fluorogenic substrates Suc-LLVY-AMC (for chymotrypsin-like activity), Z-LLE-AMC (for peptidylglutamyl peptide hydrolyzing (PGPH) activity) and Z-ARR-AMC (for trypsin-like activity) as described previously [30]. Treated cells were suspended in 50 mM Tris–HCl/pH7.4 containing 5 mM EDTA, 150 mM NaCl, 0.5% Nonidet P-40, 5 mM ATP, 0.5 mM phenylmethylsulfonyl fluoride, and 0.5 mM dithiothreitol. The cell suspensions were incubated on ice for 30 min with vigorous vortexing every 10 min for 10 s. After centrifugation, the equal amounts of protein from each sample were incubated with each substrate (20 μM, final concentration) for 30 min at 37 °C in 100 μL of the assay buffer (50 mM Tris–HCl, pH7.4). Each proteasomal activity was monitored by measuring fluorescence of hydrolyzed AMC groups using a Tecan Infinite® 200 PRO multimode reader with excitation and emission setting of 380 and 460 nm, respectively.

2.11. Statistical analysis

Results are expressed as the mean values ± standard deviation (SD) and were analyzed statistically with analysis of variance (ANOVE), and differences between groups were assessed with the Tukey's method. A value of $p < 0.05$ was considered to be statistically significant.

3. Results

3.1. ***PL-0N*** *was the most potent one among the* ***PL*** *analogs in inhibiting NO and* PGE_2 *production in LPS-stimulated RAW264.7 cells*

Results from the MTT assay showed that among the test compounds, **PL-0N** possessed the highest cytotoxicity against RAW264.7 cells, but was not cytotoxic up to 2.5 μM (Fig. 2A). Accordingly, we chose the concentrations ranging from 0.1 to 2.5 μM for each compound to test the anti-inflammatory activity in LPS-stimulated RAW264.7 cells, a model of inflammation. Using the nitrite assay, we initially evaluated the inhibitory effects of **PL** and its analogs on the LPS-induced NO (an inflammatory mediator) production. As shown in Fig. 2B, treatment with LPS alone induced a considerable production of NO, which was dose-dependently inhibited by **PL**, **PL-0N**, **PL-Ben** and **PL-CA**. Among the four compounds, **PL-Ben** and **PL-CA** had effects similar to those of the parent molecule, and, as expected, **PL-0N** presented the highest activity with the inhibitory rates of 80, 50, 25 and 7% at 2.5, 1.0, 0.5 and 0.1 μM, respectively. In contrast, both **PL-01** and **PL-02** were inactive in inhibiting the LPS-stimulated NO production, indicating that either of the two Michael acceptor units is essential for anti-inflammatory activity of **PL**. Furthermore, the structure-activity relationship (SAR) of **PL** and its analogs in inhibiting PGE_2 (another inflammatory mediator) production was in agreement with that obtained in inhibiting NO production, and **PL-0N** again ranked top among the test compounds (Fig. 2C). Based on the above experiments, we subsequently selected the concentrations of 1.0 and 2.5 μM to further probe anti-inflammatory mechanisms of **PL** and **PL-0N.**

The iNOS and COX-2 are the key enzymes involved in stimulus-induced synthesis of NO and PGE_2, respectively [31,32]. Therefore, we detected the expression of iNOS and COX-2 in LPS-stimulated RAW264.7 cells using immunoblot. As shown in Fig. 2D, the LPS-mediated induction of iNOS and COX-2 proteins was dose-dependently suppressed by **PL** or **PL-0N**, and, noticeably, the former was completely inhibited in the presence of 2.5 μM **PL-0N**. Based on these observations, we can conclude that compared with **PL**, **PL-0N** exerts the increased inhibitory effects on production of NO and PGE_2 through suppression of expression of iNOS and COX-2 in LPS-induced RAW264.7 macrophages.

3.2. ***PL-0N*** *exhibited potent inhibitory effect on nuclear translocation of NF-κB in LPS-stimulated RAW264.7 cells*

To gain an insight into the mechanisms by which both the compounds inhibit inflammation process, we sought to determine whether disruption of the distribution of NF-κB was involved in this process. Based on immunofluorescence analysis (Fig. 3A), NF-κB subunit P65 was almost exclusively observed in the cytoplasm

Please cite this article in press as: Sun L-D, et al. Development and mechanism investigation of a new piperlongumine derivative as a potent anti-inflammatory agent. Biochem Pharmacol (2015), http://dx.doi.org/10.1016/j.bcp.2015.03.014

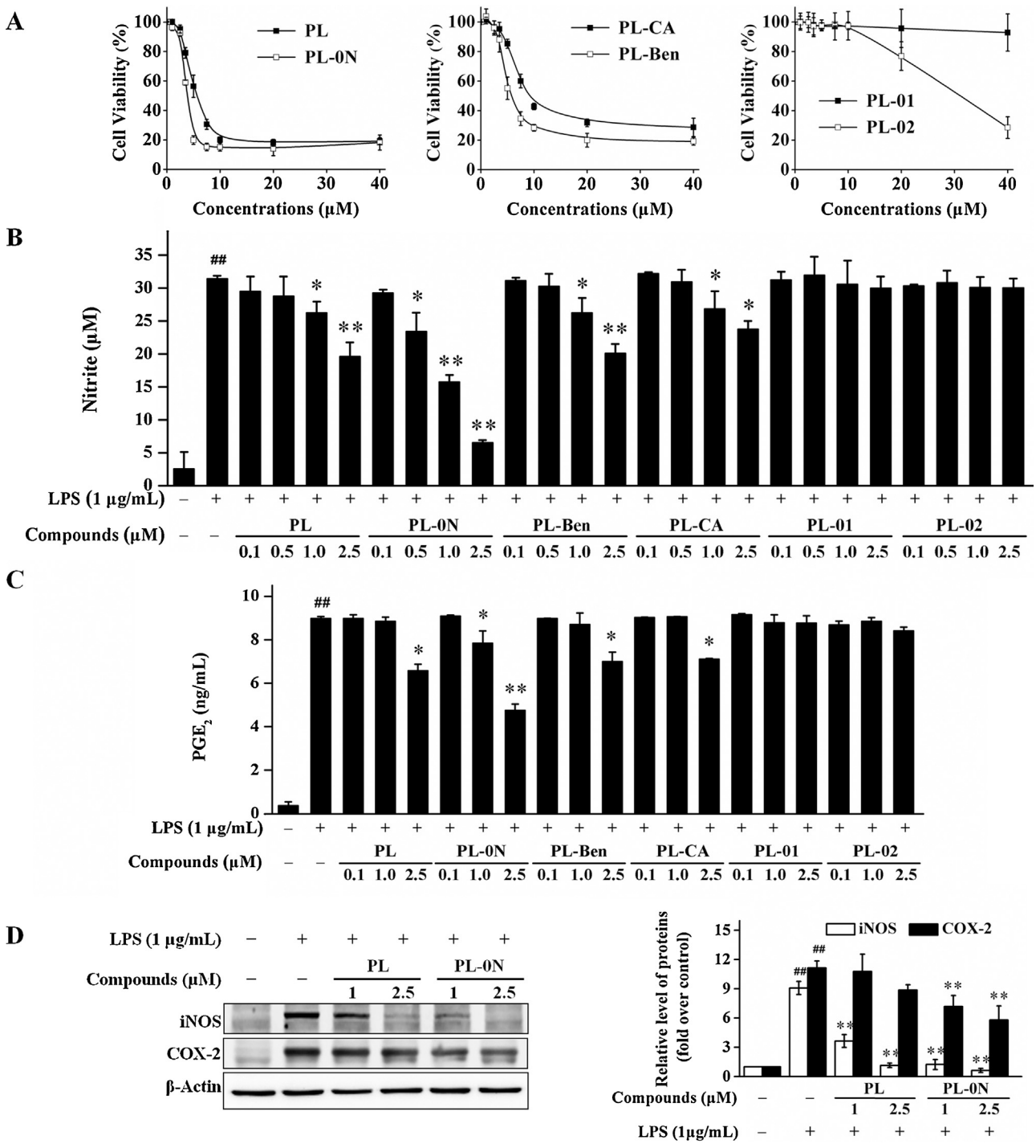

Fig. 2. Among the test compounds, **PL-0N** was the most potent one in inhibiting production of NO and PGE_2 in LPS-stimulated RAW264.7 cells. (A) Cells were treated with 0.1, 1.0, 2.5, 3.5, 5.0, 7.5, 10.0, 20.0 and 40.0 μM PL or its analog for 24 h and cell viability was analyzed using the MTT method. (B and C) Cells were treated with **PL** and its analogs for 1 h, followed by stimulation with LPS for another 18 h (B) or 24 h (C). At the end of incubation time, concentrations of NO and PGE_2 in the culture medium were quantified by nitrite and ELISA assay, respectively. (D) Cells were pretreated with different concentrations of **PL** or **PL-0N** for 1 h, LPS was then added and incubated for 24 h. The expression of iNOS, COX-2 and β-Actin was analyzed by Western blot. Results are the mean ± SD, for the NO assay, $n = 5$, other experiments, $n = 3$. ## $p < 0.01$, vs. Contol. * $p < 0.05$, ** $p < 0.01$, vs. LPS alone.

in the un-stimulated cells. After stimulation with LPS for 1 h, most cytoplasmic p65 was translocated into the nucleus. Nuclear localization of p65 was significantly reduced by **PL-0N** at all concentrations examined (Fig. 3A). Similar result was also found with 2.5 μM **PL**, but no inhibitory effect appeared at 1 μM (Fig. 3A). Consistent with these findings, immunoblot showed that the levels of both p65 and p50 were significantly increased in nuclear after LPS-induction for 30 min, which were prevented by **PL** and **PL-0N** in a concentration-dependent manner (Fig. 3B). These data indicates that the two compounds have the ability to inhibit nuclear translocation of NF-κB.

3.3. *PL-0N effectively inhibited the LPS-induced phosphorylation of IKKα/β and IκBα and impaired the proteasome activity in RAW264.7 cells*

Stimulation with LPS activates the IKK complex, leading to the phosphorylation and degradation of IκB and permitting

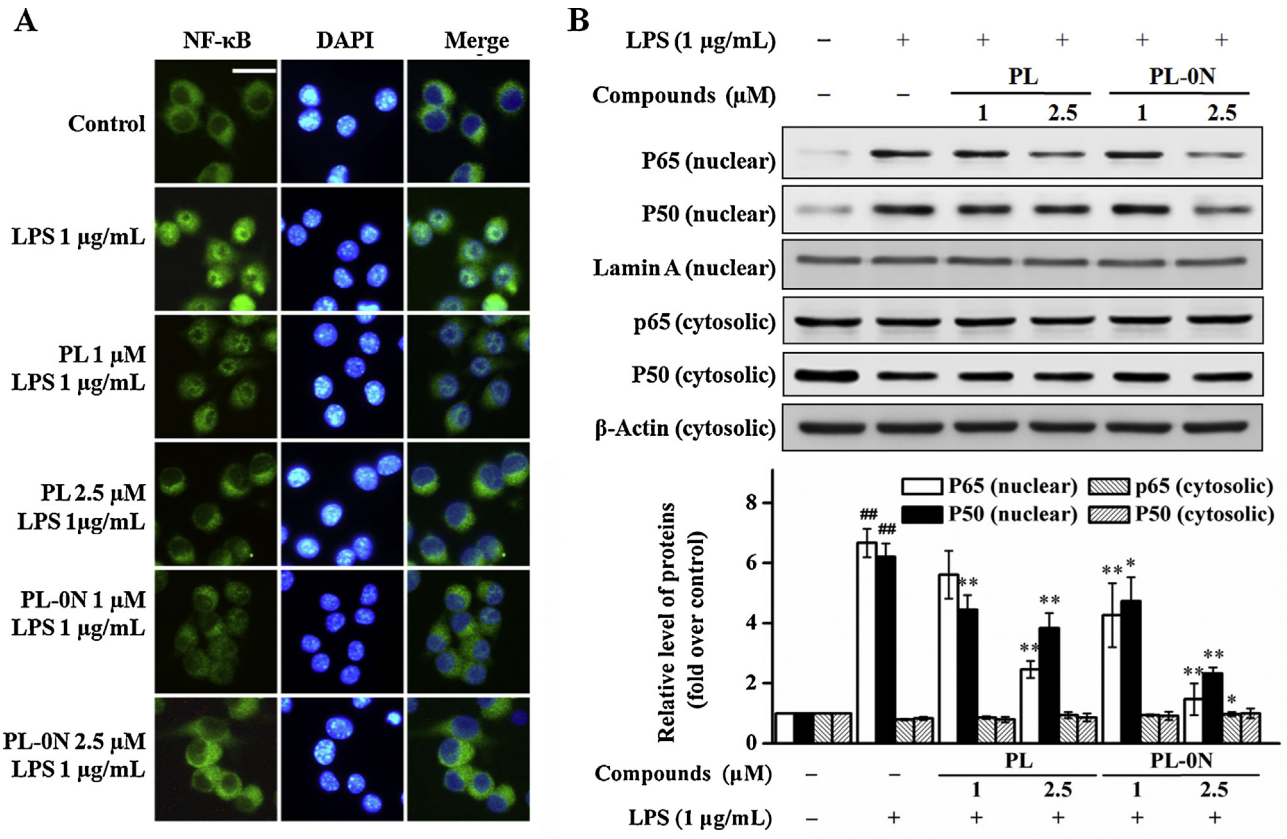

Fig. 3. PL-0N exhibited potent inhibitory effect on nuclear translocation of NF-κB in LPS-stimulated RAW264.7 cells. Cells were treated with **PL** or **PL-0N** for 5 h, followed by stimulation with LPS for 1 h (A) or 30 min (B). The subcellular localization of NF-κB was determined by immunofluorescence and images were acquired using a Leisa DM4000 B fluorescence microscope (Scale bar: 15 μm) (A). The cytosolic and nuclear fractions were prepared and analyzed by Western blotting (B). Results are the mean ± SD, $n = 3$. ## $p < 0.01$, vs. Contol. * $p < 0.05$, ** $p < 0.01$, vs. LPS alone. (Concerning the original color figure, please see the web version of this article).

translocation of NF-κB to the nucleus. Thus, we analyzed the effects of **PL** and **PL-0N** on LPS-induced IKKα/β activation and IκBα degradation by immunoblotting. In response to LPS stimulation, phosphorylated IKKα/β and IκBα levels were markedly increased, and IκBα protein expression was correspondingly diminished (Fig. 4A and B). **PL** and **PL-0N** markedly blocked LPS-induced phosphorylation of IKKα/β and IκBα as well as degradation of IκBα in a concentration-dependent manner (Fig. 4A and B). Noticeably, the LPS-induced IKKα/β phosphorylation was entirely suppressed by pretreatment with 2.5 μM **PL-0N** (Fig. 4A).

In addition, IκB stability is regulated by ubiquitin-mediated proteasomal degradation pathway. To determine whether **PL-** and **PL-0N-**induced attenuation of IκB degradation is related to impairment of proteasome activity, we detected various peptidase activities associated with the 20S proteasome. As shown in Fig. 4C, chymotrypsin, trypsin-like and PGPH activities were significantly decreased in the cells treated with 2.5 μM **PL-0N** as compared with that in the untreated cells. In contrast, **PL** at indicated concentrations was inactive in decreasing activities for all three 20S peptidases examined (Fig. 4C). This outcome is also in accordance with the previous observation of inactivity of **PL** in inhibiting chymotrypsin-like activity of 26S proteasome [33]. Taken together, these results demonstrate that **PL-0N** strongly prevents the NF-κB signaling by inhibiting LPS-induced IKKα/β activation and impairing proteasomal activity, thereby maintaining IκB stability in RAW264.7 cells.

3.4. *PL-0N suppressed the LPS-induced MAPK phosphorylation in macrophages*

MAPKs are also known to participate in regulating inflammation process [34]. To clarify the role of MAPKs in LPS-induced iNOS and COX-2 expression, the macrophages were challenged by LPS for 24 h in the presence or absence of three specific pharmacological antagonists SB203580, U0126, and SP600125 for activation of p38, ERK and JNK, respectively. Fig. 5A shows that all the three inhibitors could suppress LPS-induced over-expression of iNOS and COX-2, implying that all the three kinases are indeed involved in the inflammatory response. We next investigated the effect of **PL** and **PL-0N** on MAPKs in LPS-stimulated macrophages. It can be seen from Fig. 5B–D that LPS induced a sharp increase in the phosphorylation levels of p38, JNK and ERK1/2 in the cells. Pretreatment with **PL** or **PL-0N** blocked significantly the increased phosphorylation of p38 and JNK at 2.5 μM, but only marginally for p-ERK. These results suggest that **PL-0N** and **PL** mitigate LPS-induced over-expression of iNOS and COX-2 partially through inhibition of MAPK signaling pathway.

3.5. *PL-0N appeared not to affect LPS-induced TAK1-TAB1 complex formation and TAK1 activation in RAW264.7 cells*

Transforming growth factor β-activated kinase 1 (TAK1) is the upstream signaling molecule of IKK and MAPKs and its activation is mediated through a complex formation between TAK1 and TAK1-binding protein (TAB) adaptor proteins including TAB2 [35]. Thus, we examined whether **PL** and **PL-0N** interfered with the formation of the TAK1-TAB2 complex and phosphorylation of TAK1 in LPS-induced RAW264.7 cells. Immunoprecipitation and immunoblotting analyses show that TAB2 and TAK1 formed a stronger complex in macrophages derived from the LPS group relative to the control (Fig. 6A). Neither **PL** nor **PL-0N** exhibited appreciable effect on LPS-induced TAK1–TAB2 complex formation (Fig. 6A). For TAK1 phosphorylation, LPS induced an increase in p-TAK1 expression

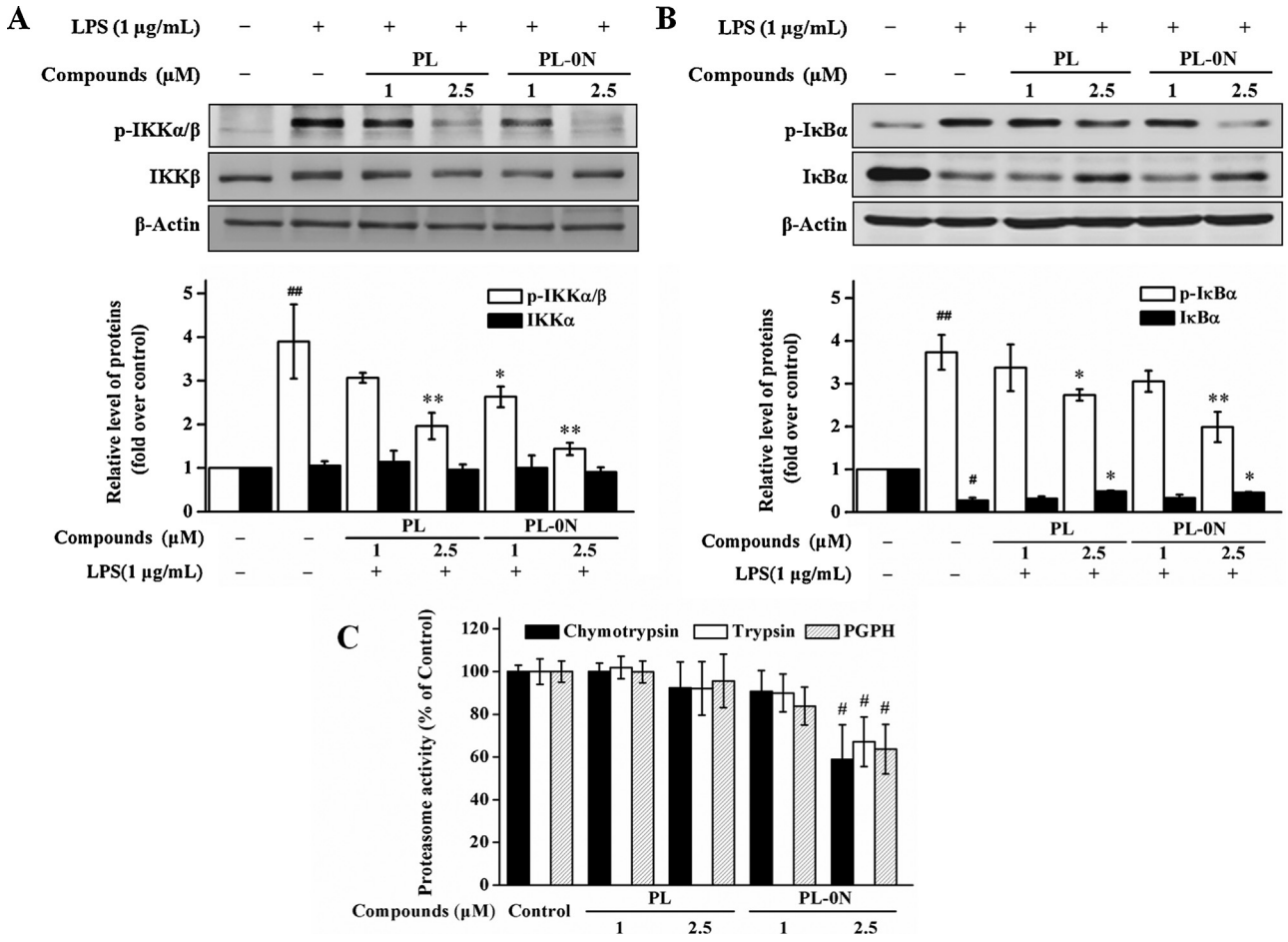

Fig. 4. PL-0N effectively inhibited the LPS-induced phosphorylation of IKKα/β and IκBα and impaired the proteasome activity in RAW264.7 cells. (A and B) Cells were pretreated with different concentrations of **PL** or **PL-0N** for 5 h, LPS was then added and incubated for another 10 min for p-IKKα/β and IKKβ or 15 min for p-IκBα and IκBα. Total cellular proteins were prepared and analyzed by Western blotting. (C) Cells were treated with indicated concentrations of **PL-0N** and **PL** for 5 h and then collected and processed for proteasome activity assay as described in Section 2. Results are the mean ± SD, $n = 3$. # $p < 0.05$, ## $p < 0.01$, vs. Contol. * $p < 0.05$, ** $p < 0.01$, vs. LPS alone.

and pre-incubation with **PL** and **PL-0N** failed to inhibit the increase at the indicated concentrations (Fig. 6B), suggesting that anti-inflammatory activity of **PL** and **PL-0N** is independent of p-TAK1 suppression.

3.6. *PL-0N strongly inhibited LPS-induced DNA binding of NF-κB in LPS-stimulated RAW264.7 cells*

Although inhibition of NF-κB activation can be achieved at various steps along NF-κB signaling, the direct suppression of DNA binding of NF-κB is a more attractive approach in inhibiting NF-κB activation [36]. Thus, we applied EMSA assay, a technique used to detect protein complexes with nucleic acids, to investigate whether **PL-0N** and **PL** is able to inhibit the DNA binding of NF-κB. As shown in Fig. 7, LPS stimulated a rapid increase in NF-κB-DNA-binding activity as indicated by forming a strong NF-κB-DNA complex band, and this activity was inhibited by 2.5 μM **PL**. At the same concentration, the inhibition effect of **PL-0N** was much more pronounced than that of **PL**. Specificity of the protein/DNA reaction was also confirmed by the finding that excess unlabeled, but not excess mutant unlabeled oligonucleotide, completely prevented the band shifts. These data indicate that inhibition of NF-κB activation by **PL** and **PL-0N** can be mediated, at least in part, by reducing formation of NF-κB-DNA complexes.

3.7. *Autophagy induced by **PL-0N** and **PL** may restrict LPS-induced inflammatory responses in RAW264.7 cells*

It has been reported that autophagy can directly regulate inflammatory responses [37]. To confirm this phenomenon, we pre-treated RAW264.7 cells with 3-MA (an autophagy inhibitor by blocking the class III PI3Ks) or rapamycin (an autophagy inducer by targeting the negative regulators against autophagy as mammalian target of rapamycin (mTOR)), followed by addition of LPS. Incubation of RAW264.7 cells with LPS led to the accumulation of microtubule-associated protein 1 light chain 3 (LC3) puncta, typical of autophagosomes. LPS-induced punctate LC3 was markedly reduced and enhanced in the presence of 3-MA and rapamycin, respectively (Fig. 8A). Moreover, the levels of LPS-induced iNOS were down-regulated upon treatment of rapamycin plus LPS, but were not changed in the presence of 3-MA plus LPS (Fig. 8B), further supporting the role of autophagy in reducing inflammatory responses in RAW264.7 cells.

Thus, it is of interest to check whether **PL** and **PL-0N** exhibit anti-inflammatory activity by influencing the LPS-induced autophagy. As illustrated in Fig. 8C, **PL** alone induced an increase in the percentage of autophagosomes in RAW264.7 cells, but to a lesser extent than **PL-0N** alone did. In comparison with treatment with LPS alone, co-treatment of LPS with either **PL-0N** or **PL** further enhanced accumulation of punctate LC3. Additionally, it can be

Please cite this article in press as: Sun L-D, et al. Development and mechanism investigation of a new piperlongumine derivative as a potent anti-inflammatory agent. Biochem Pharmacol (2015), http://dx.doi.org/10.1016/j.bcp.2015.03.014

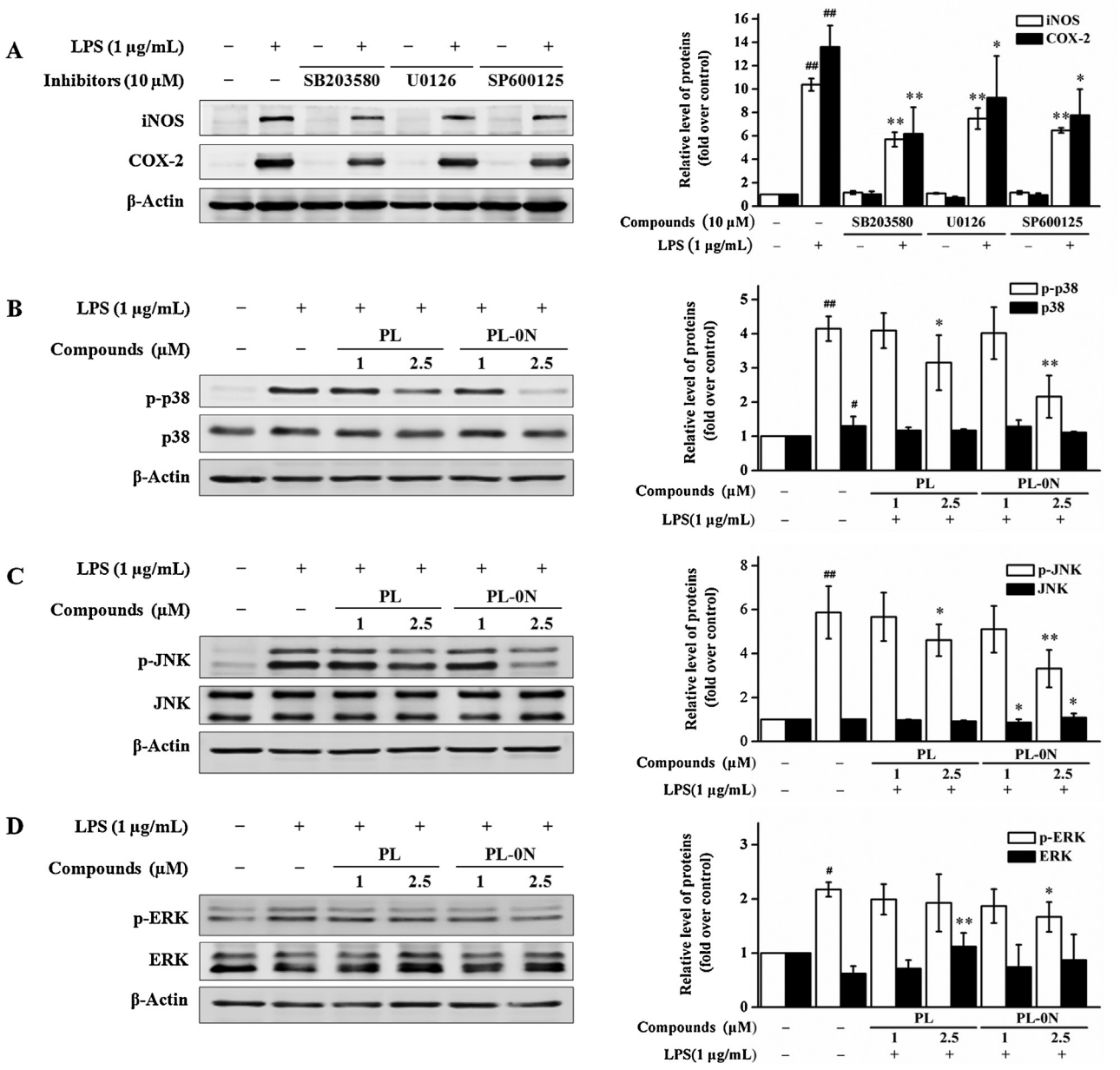

Fig. 5. PL-0N suppressed the LPS-induced MAPK phosphorylation in macrophages. (A) Roles of MAPK signaling pathways in LPS-induced macrophages. Cells were pretreated with each inhibitor for 1 h, LPS was then added and incubated for 24 h. Total cellular proteins were prepared and analyzed by Western blotting. (B–D) **PL-0N** suppressed the LPS-induced phosphorylation of p38 (B), JNK (C) and ERK1/2 (D) in macrophages. Cells were pretreated with different concentrations of **PL** or **PL-0N** for 5 h before exposure to LPS for 15 min. Total cellular proteins were prepared and analyzed by Western blotting. Results are the mean ± SD, $n = 3$. # $p < 0.05$, ## $p < 0.01$, vs. Contol. * $p < 0.05$, ** $p < 0.01$, vs. LPS alone.

seen from Fig. 8D obtained by immunoblot that **PL** or **PL-0N** alone stimulated an increase in LC3-II amount together with a reduction in p62 expression. LC3-II is considered as a marker for autophagy and p62 is widely used as an indicator of autophagic degradation [38]. Therefore, **PL** and **PL-0N** induced autophagy by initiating autophagosome formation. Considering that Akt/mTOR signaling axis is a crucial pathway to regulate the formation of autophagosomes and **PL** induces autophagy through the Akt/mTOR pathway in several cancer cells [39], we tested the effects of **PL** and **PL-0N** on levels of p-Akt and p-mTOR in RAW264.7 cells by immunoblot. Levels of p-mTOR were down-regulated by treatment with **PL** or **PL-0N**, but those of p-Akt remained unchanged (Fig. 8D). Collectively, these data imply that **PL-0N** or **PL** induces autophagy in an mTOR- rather than Akt-dependent manner and resulted in further accumulation of autophagosomes in the presence of LPS, thereby restricting LPS-induced inflammatory responses in RAW264.7 cells.

4. Discussion

Natural products, traditionally referred to as secondary metabolites, have been used for the treatment and prevention of cancer throughout history [40]. They provide extraordinarily diverse chemical scaffolds on which chemical modification can be applied to recognize the structural requirements that are responsible for the related biological activity and to derive new lead drug molecules with superior activity. Piperlongumine, a natural product, features a prominent anti-cancer activity in a broad variety of human cancer cell lines, and does not affect noncancerous cell types even at high does [12]. Subsequently, the

Please cite this article in press as: Sun L-D, et al. Development and mechanism investigation of a new piperlongumine derivative as a potent anti-inflammatory agent. Biochem Pharmacol (2015), http://dx.doi.org/10.1016/j.bcp.2015.03.014

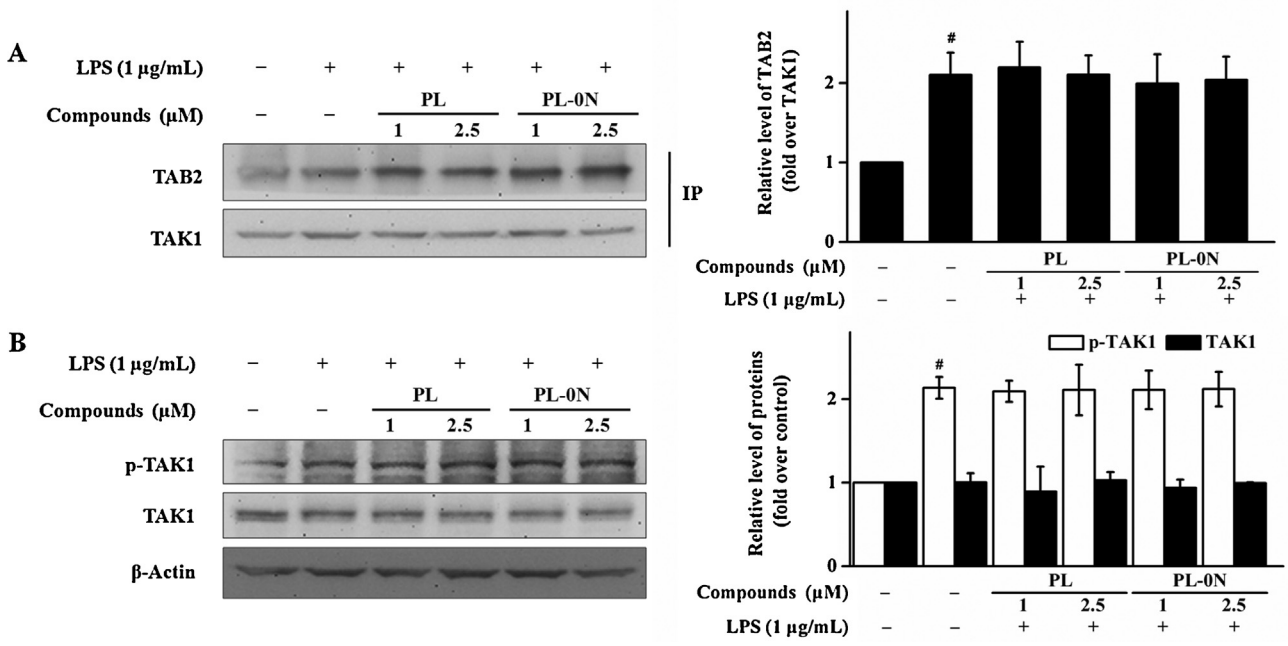

Fig. 6. PL-0N appeared not to affect LPS-induced TAK1-TAB1 complex formation and TAK1 activation in RAW264.7 cells. Cells were pretreated with the indicated concentrations of **PL** or **PL-0N** for 5 h and then challenged with LPS for 10 min. (A) Lysates were immunoprecipitated with anti-TAK1 antibody, and the immune complexes were analyzed by Western blotting using antibody against TAB2. (B) The total cellular proteins were prepared and the expression of p-TAK1, TAK1 and β-Actin was analyzed by Western blot. Results are the mean ± SD, $n = 3$. # $p < 0.05$, vs. Contol.

mechanisms of underlying its anticancer activity have been widely investigated using **PL** and/or its analogs [13–17,39]. However, there are few researches focusing on anti-inflammatory activity and mechanisms of **PL**-based analogs.

The present work studied anti-inflammatory activity of six PL-based analogs (Fig. 1A) with different structural features that enable us to clarify the structural determinants for the activity and a SAR. Specifically, either of the two Michael acceptors in **PL** is indispensible for its anti-inflammatory activity (Fig. 2B and C). This result is also in line with the previous observation showing that both the olefins are necessary to recapitulate the level of cytotoxicity observed for **PL** [18]. On the other hand, removal of either the methoxyl group or the aromatic ring has no appreciable effect on anti-inflammatory activity of **PL**. Notably, a replacement of nitrogen atom of lactam by carbon atom increases the NO- and PGE_2-inhibiting activity of **PL** (Fig. 2B and C), thereby indicating that the structural modification based on the electrophilicity-increasing strategy is feasible in improving its anti-inflammatory activity.

The inflammatory cascade is triggered by various signaling pathways, among which IKK/NF-κB signaling is the most important one, and has been long identified as a major target for many anti-inflammatory agents. In this study, we identified **PL-0N**, a nitrogen-atom-lacking analog of **PL**, as a potential anti-inflammatory agent through targeting the IKK-dependent NF-κB pathway (Fig. 4A). IKK complex is the master regulator of NF-κB activation and harbors a cysteine 179 (Cys^{179}) positioned in active site of IKK catalytic subunit IKKβ [41]. This active cysteine residue can serve as a potential target of some electrophilic molecules containing Michael acceptor unit such as epoxyquinone A monomer (EqM) [42], plumbagin [43], butein [44], and parthenolide [45]. They can covalently modify Cys^{179} of IKKβ and thereby inhibit activation of IKK. In addition, in terms of its Michael acceptors, PL has been previously proven to directly interact with this active cysteine residue together with a significant inhibition on IKK activity [46]. The current work confirms that **PL-0N**, compared with **PL**, displays increased inhibitory effect on phosphorylation of IKKα/β (Fig. 4A), resulting in subsequent failure in phosphorylation of

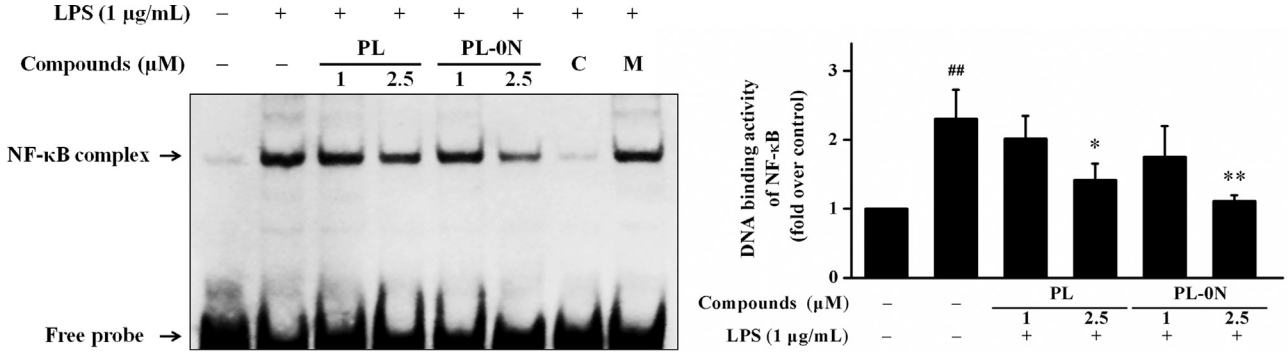

Fig. 7. PL-0N strongly inhibited LPS-induced DNA binding of NF-κB in LPS-stimulated RAW264.7 cells. Cells were pretreated with the indicated concentrations of **PL** or **PL-0N** for 5 h and then challenged with LPS for 30 min. Nuclear extract proteins (10 μg) were prepared and analyzed by EMSA assay. NF-κB complex and excessive probe are indicated by arrows. The lanes designated "C" show the effect of adding excess unlabeled NF-κB oligonucleotide; "M", the effect of adding excess unlabeled mutant NF-κB oligonucleotide.

Please cite this article in press as: Sun L-D, et al. Development and mechanism investigation of a new piperlongumine derivative as a potent anti-inflammatory agent. Biochem Pharmacol (2015), http://dx.doi.org/10.1016/j.bcp.2015.03.014

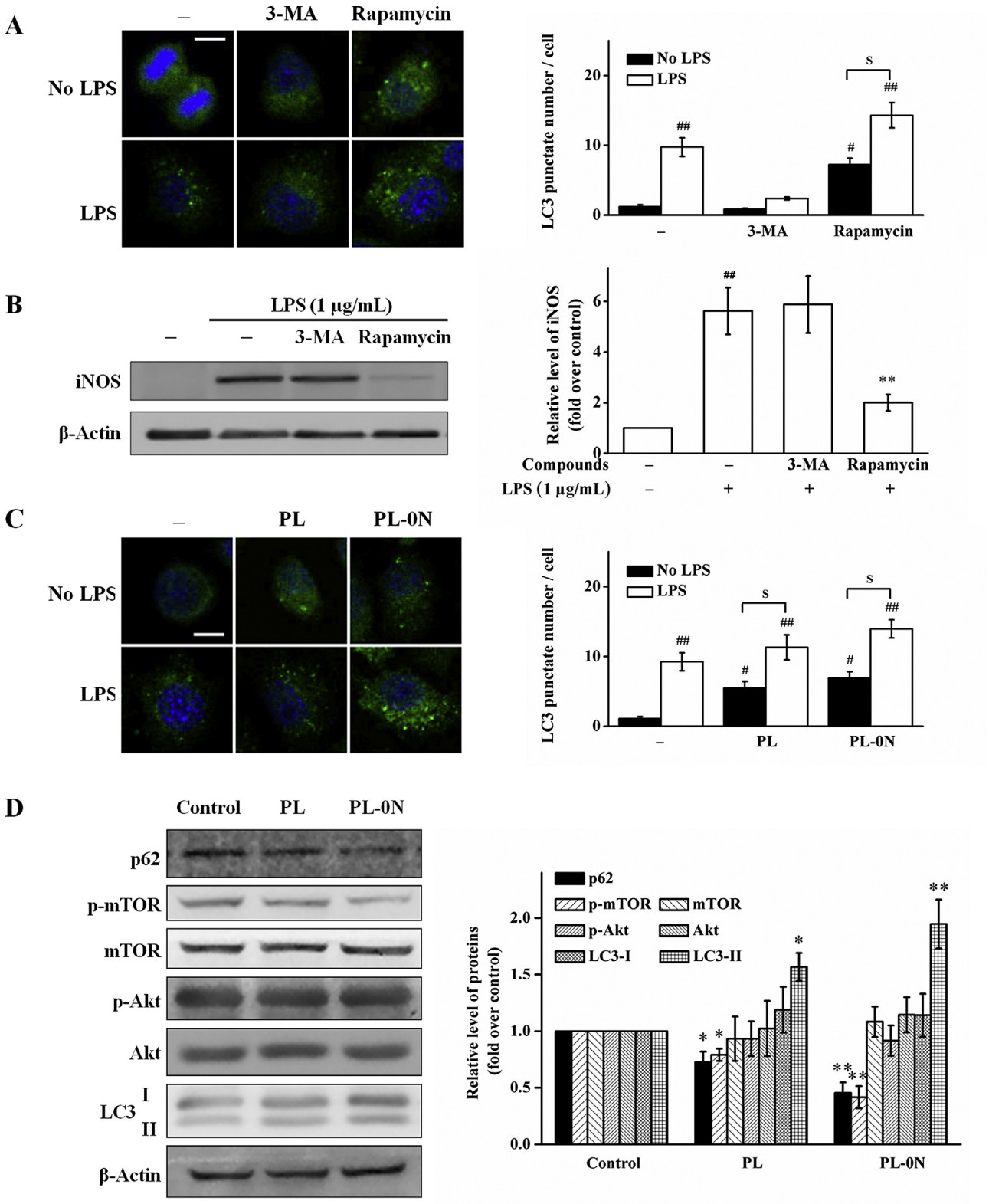

Fig. 8. Autophagy induced by **PL-0N** and **PL** may restrict LPS-induced inflammatory responses in RAW264.7 cells. (A) LPS induced autophagy in RAW264.7 cells. Cells were incubated with 1 mM 3-MA or 10 μM Rapamycin in the absence or presence of LPS (1 μg/mL) for 16 h. Then immunofluorescence for LC3 was visualized using a Zeiss LSM 710 confocal microscope (left panel) and quantified by LC3 puncta per cell (right panel). (B) Autophagy may restrict expression of iNOS in LPS-induced RAW264.7 cells. Cells were pretreated with 1 mM 3-MA or 10 μM rapamycin for 30 min, and incubated for 24 h after addition of LPS. Total cellular proteins were prepared and analyzed by Western blotting. (C) **PL-0N** and **PL** enhanced the LPS-induced autohagy. Cells were incubated with 2.5 μM of either **PL** or **PL-0N** with or without LPS (1 μg/mL) for 16 h. Then immunofluorescence for LC3 was captured (left panel) and quantified by LC3 puncta per cell (right panel). (D) **PL** and **PL-0N** promote autophagy in an mTOR-dependent manner. Cells were incubated with 2.5 μM of either **PL** or **PL-0N** for 24 h, then the total cellular proteins were prepared. The expression of p62, p-mTOR, mTOR, p-Akt, Akt, LC3 and β-Actin was analyzed by Western blot. Results are the mean ± SD, $n = 3$. # $p < 0.05$, ## $p < 0.01$, vs. Contol. ** $p < 0.01$, vs. LPS alone. s $p < 0.05$. For D, * $p < 0.05$, ** $p < 0.01$, vs. Control. Scale bars = 10 μm. (For this figure in color, please see the web version of this article).

Please cite this article in press as: Sun L-D, et al. Development and mechanism investigation of a new piperlongumine derivative as a potent anti-inflammatory agent. Biochem Pharmacol (2015), http://dx.doi.org/10.1016/j.bcp.2015.03.014

IκBα and nuclear entry of p65 and p50. Consequently, Cys^{179} of IKKβ probably serves as an interaction site for **PL-0N** based on its structural and functional similarities to that of **PL**. Apart from Cys^{179} of IKKβ, Cys^{38} in p65 and Cys^{62} in p50 have been recognized as the attachment sites of a few electrophiles as exemplified by EqM [42], plumbagin [43] and andrographolide [47]. The direct interaction with both p65 and p50 reduces generally the binding affinity of NF-κB toward DNA [36,42,43,47]. As demonstrated by EMSA analysis (Fig. 7), both **PL** and **PL-0N** inhibited obviously the NF-κB-DNA binding activity stimulated by LPS, and the inhibitory activity of the latter is superior to that of the former, suggesting the possibility of their targeting Cys^{38} in p65 or Cys^{62} in p50 or both of them. Taken together, their anti-inflammatory activity is closely associated with their ability to inhibit IKK phosphorylation and the NF-κB-DNA binding.

In inflammatory process, the ubiquitin-proteasome pathway plays an important role since it regulates activation of IKK and degradation IκB as well as processing of the NF-κB precursors, p100 and p105, in to the mature subunits p52 and p50 [48]. It is not surprising that proteasome inhibitors, such as epoxomicin, cyclosporine A, can inhibit NF-κB activation [49,50]. In this work, inhibition of 20S proteosomal activity is observed only in the case of 2.5 μM **PL-0N** instead of **PL**. It appears likely that the enhanced anti-inflammatory activity of **PL-0N** is due, at least in part, to its ability to impair proteasome activity.

MAPKs, including p38, ERK1/2 and JNK subgroups, are a highly conserved family of protein serine/threonine kinases involved in a variety of fundamental cellular processes. These three MAPKs are known to play an important role in regulating LPS-induced inflammation responses [34]. Fig. 5 confirms that p38, ERK1/2 and JNK are involved in LPS-induced inflammation responses, and their phosphorylation (especially p-p38 and p-JNK) inhibition contributes to anti-inflammatory activity of **PL** and **PL-0N.**

TAK1, a member of the MAPKKK family, is an indispensable signaling intermediate in LPS/toll-like receptor (TLR)4 signaling pathway. Following LPS stimulation, TLR4 activates myeloid differentiation protein 88 (MyD88)-dependent pathway and leads to TAK1-TAB2 complex formation, TAK1 activation, and subsequent activation of IKK and MAPKs [51–53]. It can be seen from Fig. 6 that neither **PL** nor **PL-0N** interferes with formation of TAK1-TAB2 complex and TAK1 phosphorylation in LPS-induced RAW264.7 cells, suggesting that TAK1 and its upstream molecules including TLR4 should not be affected by **PL** or **PL-0N**. There should be other targets contributing to down-regulation of **PL** and **PL-0N** for the LPS-induced phosphorylated MAPKs.

Autophagy is a regulated bulk degradation process inside cells, and contributes to the turnover of cellular components. A recent wave of interest in autophagy has been characterized by its involvement in regulating inflammatory responses [37]. Using Atg16L1-deficiency mice, Saitoh et al. found that autophagy dysregulation enhances endotoxin-induced production of IL-1β [54]. In contrast, we found that rapamycin is able to significantly decrease LPS-induced iNOS expression (Fig. 8B). Furthermore, Fig. 8C shows that anti-inflammatory activity of **PL** and **PL-0N** can be partly due to inducing autophagy. In fact, NF-κB activation in LPS-activated cells is inversely correlated to the enhancement of

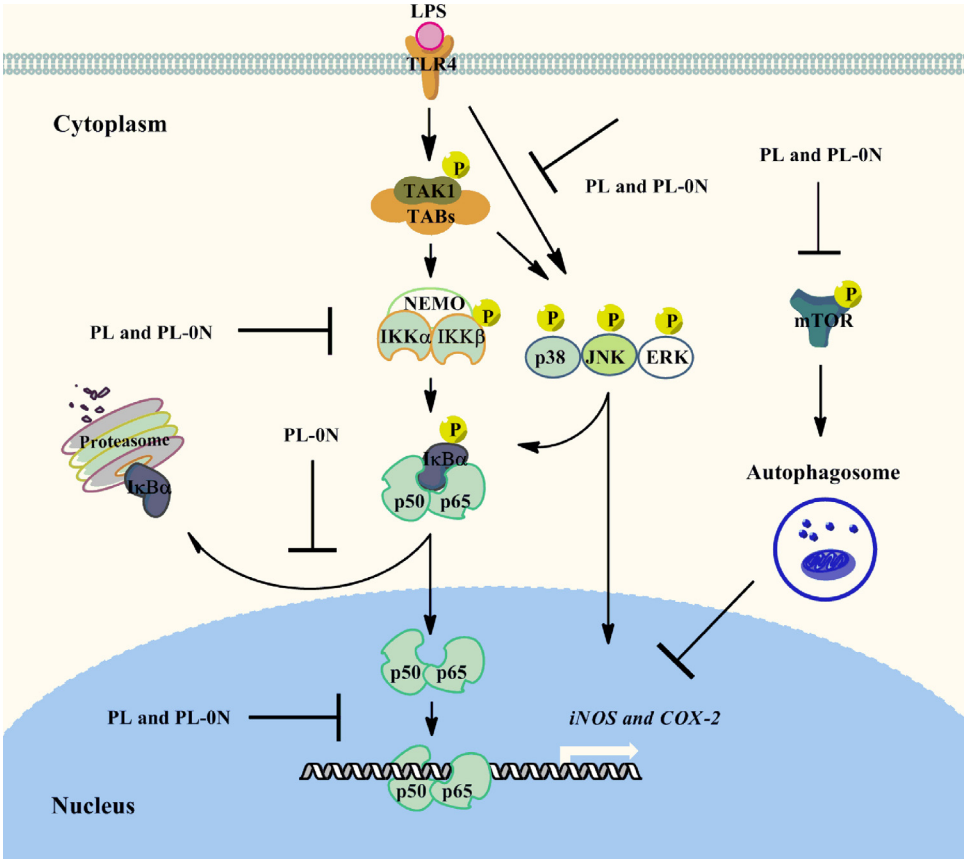

Fig. 9. Schematic diagram showed the molecular mechanism through which **PL** and **PL-0N** inhibit LPS-induced inflammatory process in LPS-induced RAW264.7 cells. In response to LPS stimulation, IKK, p38, ERK and JNK becomes activated. After activation, the IKK complex phosphorylates IκBα, which is then ubiquitinated and degraded by 20S proteasome, thereby leading to the activation of NF-κB and subsequent transcription of iNOS and COX-2. Each of these events can be blocked by **PL** and **PL-0N** with one exception that the former is inactive in impairing proteasome activity. Besides, induction of autophagy by **PL** and **PL-0N** also contributes to their anti-inflammatory activity. The Cys^{179} of IKKβ, Cys^{38} in p65 and Cys^{62} in p50 are possible attachment sites of PL and PL-0N in terms of their Michael acceptors (see Section 4). P, phosphate group; ⊥, site of inhibition. (Concerning this illustration in color, please see the web version of this article).

Please cite this article in press as: Sun L-D, et al. Development and mechanism investigation of a new piperlongumine derivative as a potent anti-inflammatory agent. Biochem Pharmacol (2015), http://dx.doi.org/10.1016/j.bcp.2015.03.014

autophagy. Moreover, NF-κB provides a molecular link between autophagy and its function in suppressing inflammation [55]. Autophagy selectively degrades NF-κB-inducing kinase (NIK) and IKK, resulting in attenuation of NF-κB activation [56,57], while activated NF-κB represses autophagy activation induced by TNF-α [58]. In view of the fact that NF-κB is a key regulator in inflammation responses and autophagy degrades NIK and IKK, we postulate that anti-inflammatory activity of **PL** and **PL-0N** is primarily mediated by inhibiting NF-κB activation, and the autophagic induction by them in an mTOR-dependent manner further contributes to this inhibition.

In conclusion, by using a LPS-stimulated RAW264.7 cell model, we identified **PL-0N**, a nitrogen-atom-lacking analog of **PL**, as a promising lead for developing natural product-directed anti-inflammatory agents, and revealed its anti-inflammatory mechanisms including inhibition of NF-κB transduction pathway, down-regulation of MAPKs activation, impairment of proteasome activity and induction of autophagy (Fig. 9). Additionally, this work highlights the feasibility in designing **PL**-inspired anti-inflammatory agents by the electrophilicity-increasing strategy.

Acknowledgements

This work was supported by the National Natural Science Foundation of China (grant no. 21372109), and the 111 Project.

References

[1] N.C. Walsh, T.N. Crotti, S.R. Goldring, E.M. Gravallese, Rheumatic diseases: the effects of inflammation on bone, Immunol. Rev. 208 (2005) 228–251.
[2] P. Libby, P.M. Ridker, A. Maseri, Inflammation and atherosclerosis, Circulation 105 (2002) 1135–1143.
[3] M. Karin, Nuclear factor-κB in cancer development and progression, Nature 441 (2006) 431–436.
[4] S. Ghosh, M.S. Hayden, New regulators of NF-κB in inflammation, Nat. Rev. Immunol. 8 (2008) 837–848.
[5] P.J. Barnes, M. Karin, Nnuclear factor-κB—a pivotal transcription factor in chronic inflammatory diseases, N. Engl. J. Med. 336 (1997) 1066–1071.
[6] P.A. Baeuerle, V.R. Baichwal, NF-κB as a frequent target for immunosuppressive and anti-inflammatory molecules, Adv. Immunol. 65 (1997) 111–137.
[7] S. Ghosh, M.J. May, E.B. Kopp, NF-κB and Rel proteins: evolutionarily conserved mediators of immune responses, Annu. Rev. Immunol. 16 (1998) 225–260.
[8] T. Henkel, U. Zabel, K. van Zee, J.M. Müller, E. Fanning, P.A. Baeuerle, Intramolecular masking of the nuclear location signal and dimerization domain in the precursor for the p50 NF-κB subunit, Cell 68 (1992) 1121–1133.
[9] P. Bremner, M. Heinrich, Natural products as targeted modulators of the nuclear factor-κB pathway, J. Pharm. Pharmacol. 54 (2002) 453–472.
[10] S.I. Grivennikov, F.R. Greten, M. Karin, Immunity, inflammation, and cancer, Cell 140 (2010) 883–899.
[11] M. Gersch, J. Kreuzer, S.A. Sieber, Electrophilic natural products and their biological targets, Nat. Prod. Rep. 29 (2012) 659–682.
[12] L. Raj, T. Ide, A.U. Gurkar, M. Foley, M. Schenone, X.Y. Li, et al., Selective killing of cancer cells by a small molecule targeting the stress response to ROS, Nature 475 (2011) 231–234.
[13] E.H. Kong, Y.J. Kim, Y.J. Kim, H.J. Cho, S.N. Yu, K.Y. Kim, et al., Piplartine induces caspase-mediated apoptosis in PC-3 human prostate cancer cells, Oncol. Rep. 20 (2008) 785–792.
[14] Q.R. Liu, J.M. Liu, Y. Chen, X.Q. Xie, X.X. Xiong, X.Y. Qiu, et al., Piperlongumine inhibits migration of glioblastoma cells via activation of ROS-dependent p38 and JNK signaling pathways, Oxid. Med. Cell Longev. (2014), http://dx.doi.org/10.1155/2014/653732.
[15] H. Randhawa, K. Kibble, H. Zeng, M.P. Moyer, K.M. Reindl, Activation of ERK signaling and induction of colon cancer cell death by piperlongumine, Toxicol. In Vitro 27 (2013) 1626–1633.
[16] S.S. Han, D.J. Son, H. Yun, N.L. Kamberos, S. Janz, Piperlongumine inhibits proliferation and survival of Burkitt lymphoma in vitro, Leuk. Res. 37 (2013) 146–154.
[17] S. Ginzburg, K.V. Golovine, P.B. Makhov, R.G. Uzzo, A. Kutikov, V.M. Kolenko, Piperlongumine inhibits NF-κB activity and attenuates aggressive growth characteristics of prostate cancer cells, Prostate 74 (2014) 177–186.
[18] D.J. Adama, M.J. Dai, G. Pellegrino, B.K. Wagner, A.M. Stern, A.F. Shamji, et al., Synthesis, cellular evaluation, and mechanism of action of piperlongumine analogs, Proc. Natl. Acad. Sci. U.S.A. 109 (2012) 15115–15120.
[19] Z.V. Boskovic, M.M. Hussain, A.J. Adams, M.J. Dai, S.L. Schreiber, Synthesis of piperlogs and analysis of their effects on cells, Tetrahedron 69 (2013) 7559–7567.
[20] G.Y. Liu, J. Yang, F. Dai, W.J. Yan, Q. Wang, X.Z. Li, et al., CuII ions and the stilbene-chroman hybrid with a catechol moiety synergistically induced DNA damage, and cell cycle arrest and apoptosis of HepG2 cells: an interesting acid/base-promoted prooxidant reaction, Chem. Eur. J. 18 (2012) 11100–11106.
[21] Y.F. Kang, W.J. Yan, T.W. Zhou, F. Dai, X.Z. Li, X.Z. Bao, et al., Tailoring 3,3′-dihydroxyisorenieratene to hydroxystilbene: finding a resveratrol analogue with increased antiproliferation activity and cell selectivity, Chem. Eur. J. 20 (2014) 8904–8908.
[22] D.K. Winter, A. Drouin, J. Lessard, C. Spino, Photochemical rearrangement of *N*-chlorolactams: a route to *N*-heterocycles through concerted ring contraction, J. Org. Chem. 75 (2010) 2610–2618.
[23] J.X. Gu, H.L. Holland, A convenient synthesis of 3-arylbutanolides and 3-arylbutenolides, Synth. Commun. 28 (1998) 3305–3315.
[24] A.E. Walts, W.R. Roush, A stereorational total synthesis of (−)-ptilocauln, Tetrahedron 41 (1985) 3463–3478.
[25] Zou Y, Sun J, Zhang KY, Ding WX, Gao L, Wu YP, inventor; Guangzhou INST of Chemistry, assignee. 4-aryl coumarin compound and preparation method and application. Chinese patent No: CN 101967315B, 20130403.
[26] Yu MH, Gao Y, inventor; Okeanos Technology Co. Ltd., assignee. Method for synthesizing piperlongumine compounds. Chinese patent No: CN 101774875A, 20100714.
[27] Li QG, Quan JP, Chen X, Wang T, Yuan P, Luo X, et al. inventor; Chongqing Medical University INST of Medicine, assignee. Process for preparing cinepazide maleate. Chinese patent No: CN 101723918B, 20110831.
[28] M. Casey, J.A. Donnelly, J.C. Ryan, S. Ushioda, Synthesis of bicyclic lactams using novel Schmidt reactions, Arkivoc 7 (2003) 310–327.
[29] J. Sun, X.J. Zhang, M. Broderick, H. Fein, Measurement of nitric oxide production in biological systems, Sensors 3 (2003) 276–284.
[30] S. Nam, D.M. Smith, Q.P. Dou, Ester bond-containing tea polyphenols potently inhibit proteasome activity in vitro and in vivo, J. Biol. Chem. 276 (2001) 13322–13330.
[31] D.A. Geller, T.R. Nilliar, Molecular biology of nitric oxide synthases, Cancer Metast. Rev. 17 (1998) 7–23.
[32] C.S. Williams, M. Mann, DuBois RN:, The role of cyclooxygenases in inflammation, cancer, and development, Oncogene 18 (1999) 7908–7916.
[33] M. Jarvius, M. Fryknäs, P.D. Arcy, C. Sun, L. Rickardson, J. Gullbo, et al., Piperlongumine induces inhibition of the ubiquitin-proteasome system in cancer cells, Biochem. Biophys. Res. Commun. 431 (2013) 117–123.
[34] B. Kaminska, MAPK signaling pathways as molecular targets for anti-inflammatory therapy-from molecular mechanisms to therapeutic benefits, Biochim. Biophys. Acta 1754 (2005) 253–262.
[35] C. Wang, L. Deng, M. Hong, G.R. Akkaraju, J. Inoue, Z.J. Chen, TAK1 is a ubiquitin-dependent kinase of MKK and IKK, Nature 412 (2001) 346–351.
[36] R.K. Sharma, M. Otsuka, G. Gaba, S. Mehta, Inhibitors of transcription factor nuclear factor-kappa beta (NF-κβ)-DNA binding, RSC Adv. 3 (2013) 1282–1296.
[37] B. Levine, N. Mizushima, H.W. Virgin, Autophagy in immunity and inflammation, Nature 469 (2011) 323–335.
[38] N. Mizushima, T. Yoshimori, B. Levine, Methods in mammalian autophagy research, Cell 140 (2010) 313–326.
[39] P. Makhov, K. Golovine, E. Teper, A. Kutikov, R. Mehrazin, A. Corcoran, et al., Piperlongumine promotes autophagy via inhibition of Akt/mTOR signaling and mediates cancer cell death, Br. J. Cancer 110 (2014) 899–907.
[40] N.P. Gullett, A.R. Ruhul Amin, S. Bayraktar, J.M. Pezzuto, D.M. Shin, F.R. Khuri, et al., Cancer prevention with natural compounds, Semin. Oncol. 37 (2010) 258–281.
[41] A. Israël, The IKK complex: an integrator of all signals that activate NF-κB? Trends Cell. Biol. 10 (2000) 129–133.
[42] M.C. Liang, S. Bardhan, E.A. Pace, D. Rosman, J.A. Beutler, J.A. Porco Jr., et al., Inhibition of transcription factor NF-κB signaling proteins IKKβ and p65 through specific cysteine residues by epoxyquinone A monomer: correlation with its anticancer cell growth activity, Biochem. Pharmacol. 71 (2006) 634–645.
[43] S.K. Sandur, H. Ichikawa, G. Sethi, K.S. Ahn, B.B. Aggarwal, plumbagin (5-hydroxy-2-methyl-1,4-naphthoquinone) suppresses NF-κB activation and NF-κB-regulated gene products through modulation of p65 and IκBα kinase activation, leading to potentiation of apoptosis induced by cytokine and chemotherapeutic agents, J. Biol. Chem. 281 (2006) 17023–17033.
[44] M.K. Pandey, S.K. Sandur, B. Sung, G. Sethi, A.B. Kunnumakkara, B.B. Aggarwal, Butein, a tetrahydroxychalcone, inhibits nuclear factor(NF)-κB and NF-κB-regulated gene expression through direct inhibition of IκBα Kinase β on cysteine 179 residue, J. Biol. Chem. 282 (2007) 17340–17350.
[45] B.H. Kwok, B. Koh, M.I. Ndubuisi, M. Elofeeon, C.M. Crews, The anti-infammatory natural product parthenolide from the medicinal herb Feverfew directly binds to and inhibits IκB kinase, Chem. Biol. 8 (2001) 759–766.
[46] J.G. Han, S.C. Gupta, S. Prasad, B.B. Aggarwal, Piperlongumine chemosensitizes tumor cells through interaction with cysteine 179 of IκBα kinase, leading to suppression of NF-κB-regulated gene products, Mol. Cancer Ther. 13 (2014) 2422–2435.
[47] Y.F. Xia, B.Q. Ye, Y.D. Li, J.G. Wang, He xj, F.L. Lin, et al., Andrographolide attenuates inflammation by inhibition of NF-κB activation through covalent modification of reduced cysteine 62 of p50, J. Immunol. 173 (2004) 4207–4217.
[48] S.Q. Liu, Z.J. Chen, Expanding role of ubiquitination in NF-κB signaling, Cell Res. 21 (2011) 6–21.
[49] L.H. Meng, R. Mohan, B.H.B. Kwok, M. Elofsson, N. Sin, C.M. Crews, Epoxomicin, a potent and selective proteasome inhibitor, exhibits in vivo anti-inflammatory activity, Proc. Natl. Acad. Sci. U.S.A. 96 (1999) 10403–10408.
[50] S. Meyer, N.G. Kohler, A. Joly, Cyclosporine A is an uncompetitive inhibitor of proteasome activity and prevents NF-κB activation, FEBS Lett. 413 (1997) 354–358.

Please cite this article in press as: Sun L-D, et al. Development and mechanism investigation of a new piperlongumine derivative as a potent anti-inflammatory agent. Biochem Pharmacol (2015), http://dx.doi.org/10.1016/j.bcp.2015.03.014

[51] E. Kopp, R. Medzhitov, Recognition of microbial infection by Toll-like receptors, Curr. Opin. Immunol. 15 (2003) 396–401.
[52] J. Lee, L. Mira-Arbibe, R.J. Ulevitch, TAK1 regulates multiple protein kinase cascades activated by bacterial lipopolysaccharide, J. Leukoc Biol. 68 (2000) 909–915.
[53] J. Ninomiya-Tsuji, K. Kishimoto, A. Hiyama, J. Inoue, Z. Cao, K. Matsumoto, The kinase TAK1 can activate the NIK-IkappaB as well as the MAP kinase cascade in the IL-1 signalling pathway, Nature 398 (1999) 252–256.
[54] T. Saitoh, N. Fujita, M.H. Jang, S. Uematsu, B.G. Yang, T. Satoh, et al., Loss of the autophagy protein Atg16L1 enhances endotoxin-induced IL-1β production, Nature 456 (2008) 264–268.
[55] G.T. Xiao, Autophagy and NF-κB: fight for fate, Cytokine Growth Factor. Rev. 18 (2007) 233–243.
[56] G.L. Qing, P.R. Yan, Z.X. Qu, H.D. Liu, H. Li, G.T. Xiao, Hsp90 regulates processing of NF-κB2 p100 involving protection of NF-κB-inducing kinase (NIK) from autophagy-mediated degradation, Cell Res. 17 (2007) 520–530.
[57] G.L. Qing, P.R. Yan, G.T. Xiao, Hsp90 inhibition results in autophagy-mediated proteasome-independent degradation of IκB kinase (IKK), Cell Res. 16 (2006) 895–901.
[58] M. Djavaheri-Mergny, M. Amelotti, J. Mathieu, F. Besancon, C. Bauvy, S. Souquère, et al., NF-κB activation represses tumor necrosis factor-α-induced autophagy, J. Biol. Chem. 281 (2006) 30373–30382.

Please cite this article in press as: Sun L-D, et al. Development and mechanism investigation of a new piperlongumine derivative as a potent anti-inflammatory agent. Biochem Pharmacol (2015), http://dx.doi.org/10.1016/j.bcp.2015.03.014